Published in final edited form as:
*Cell Metab*. 2007 April ; 5(4): 253–264.

# Mitochondrial GTP Regulates Glucose-Induced Insulin Secretion

**Richard G. Kibbey**[1], **Rebecca L. Pongratz**[1], **Anthony J. Romanelli**[1], **Claes B. Wollheim**[2], **Gary W. Cline**[1], and **Gerald I. Shulman**[1,3,4,*]

[1]*Department of Internal Medicine, Howard Hughes Medical Institute Yale University School of Medicine New Haven, CT 06520, USA* [3]*Department of Cellular, Howard Hughes Medical Institute Yale University School of Medicine New Haven, CT 06520, USA* [4]*Department of Molecular Physiology, Howard Hughes Medical Institute Yale University School of Medicine New Haven, CT 06520, USA* [2]*Department of Cell Physiology and Metabolism University Medical Center CH-1211 Geneva 4, Switzerland*

## Summary

Substrate-level mitochondrial GTP (mtGTP) and ATP (mtATP) synthesis occurs by nucleotide-specific isoforms of the tricarboxylic acid (TCA) cycle enzyme succinyl CoA synthetase (SCS). Unlike mtATP, each molecule of glucose metabolized produces approximately one mtGTP in pancreatic β-cells independent of coupling with oxidative phosphorylation making mtGTP a potentially important fuel signal. siRNA suppression of the GTP-producing pathway (ΔSCS-GTP) reduced glucose-stimulated insulin secretion (GSIS) by 50%, whereas suppression of the parallel ATP-producing isoform (ΔSCS-ATP) increased GSIS by two-fold in INS-1 832/13 cells and cultured rat islets. Insulin secretion correlated with increases in cytosolic calcium but not with changes in NAD(P)H or the ATP/ADP ratio. These data suggest an important role for mtGTP in mediating GSIS in β-cells by modulation of mitochondrial metabolism possibly via influencing mitochondrial calcium. Furthermore, by virtue of its tight coupling to TCA oxidation rates, mtGTP production may serve as an important molecular signal of TCA cycle activity.

## Introduction

Mitochondria generate a transmembrane potential (ΔΨ) by oxidation of carbon-based substrates in the TCA cycle. In pancreatic β-cells a portion of this potential generates ATP via oxidative phosphorylation that increases the ATP/ADP ratio and then subsequent closure of the $K_{ATP}$ channel leading to activation of voltage-dependent calcium channels (VDCC) in the plasma membrane and subsequent (canonical) glucose-induced insulin secretion (GSIS). Success of sulphonylurea reagents as pharmacologic potentiators of insulin secretion as well as mutations in the human $K_{ATP}$/SUR channel leading to either hyperinsulinemic hypoglycemia or type 2 diabetes mellitus (T2DM) underscores the importance of this channel in the regulation of GSIS. Recently, glucose induced oscillations in cytosolic calcium with corresponding insulin release were described in mice lacking $K_{ATP}$ channels questioning the central role of these channels in physiologic insulin secretion (Szollosi et al., 2007). Discovery of $K_{ATP}$-*independent* (non-canonical) mechanisms of GSIS, though less well characterized,

*To whom correspondence should be addressed. E-mail: gerald.shulman@yale.edu

have clearly identified roles for other essential signals in this process (MacDonald et al., 2005).

Since β-cell mitochondria couple glucose metabolism to insulin secretion, a seminal question is how intramitochondrial fuel metabolism is "sensed." In this regard, observations in children with hyperinsulinemia-hyperammonemia syndrome suggested a potentially important role for mitochondrial GTP (mtGTP) as such a metabolism sensor. These patients harbor mutations that impair GTP-mediated inhibition of the mitochondrial enzyme glutamate dehydrogenase (GDH) (MacMullen et al., 2001). Such mutations are associated with inappropriate hypersecretion of insulin and consequent hypoglycemia following protein-rich meals (Kelly and Stanley, 2001). Thus, impaired regulatory activity of mtGTP is clearly associated with an insulin secretory defect in humans. In addition to its control of GDH we hypothesized that mtGTP might have a broader regulatory role within the matrix to control insulin secretion.

Both ATP and GTP are metabolically generated in the matrix but their origins and fates in the mitochondrial matrix differ substantially. Mitochondrial ATP (mtATP) is produced predominantly by oxidative phosphorylation and thus is dependent on the mitochondrial membrane potential (ΔΨ) generated primarily from NADH oxidation (Fig. 1A). Only a small fraction of ATP is directly formed in the TCA cycle by the ATP isoforms of succinyl-CoA synthetase (SCS-ATP). The tightness of coupling between ΔΨ and ATP synthase determines the efficiency of ATP synthesis. In principle between 1 and 29 mtATP are generated per molecule of glucose metabolized since ΔΨ can perform work other than ATP synthesis (e.g. heat production, protein import, ion pumping, free radical generation, matrix swelling and shrinkage). Unlike the widely varying synthesis efficiency, changes in the matrix ATP/ADP ratio are relatively limited due to the rapid export of mtATP to the cytosol via the ATP/ADP transporter (AAT). Thus, at least within the matrix ATP production rates do not necessarily reflect rates of glucose oxidation. In distinct contrast, mtGTP is only metabolically generated by the GTP-specific isoform of SCS (SCS-GTP) with each subsequent turn of the TCA cycle. Assuming similar fluxes through each isoform, approximately one molecule of mtGTP will be generated per one molecule of glucose oxidized irrespective of the tightness of mitochondrial coupling. As a consequence of slow cytoplasmic exchange, metabolism-induced mtGTP is trapped in the matrix and increases in GTP/GDP are much more substantial than mtATP (Ottaway et al., 1981;Smith et al., 1974). Thus, mtGTP production is well poised to reflect TCA cycle activity.

SCS catalyzes the reversible conversion of succinyl-CoA to succinate and CoA with the generation of a purine triphosphate in the process. The two SCS isoforms share a common α-subunit but distinct β-subunits. The β-subunit confers the adenine and guanine specificities but are otherwise highly conserved in both sequence, structure, and activity (Fraser et al., 2000;Johnson et al., 1998;Weitzman et al., 1986;Wolodko et al., 1994). The ratio of isozyme activities varies with tissue type, but are similar in clonal β– cell lines (Johnson et al., 1998;Kowluru, 2001;Weitzman et al., 1986). In order to test the hypothesis that mtGTP is an intramitochondrial signal of TCA cycle activity, which in turn mediates GSIS, we selectively knocked-down the expression of the ATP-and GTP-generating isoforms of SCS, using siRNA-mediated silencing in INS-1 832/13 cells and rat islets, and assessed the impact of these perturbations on energy metabolism and GSIS.

## Results

### siRNA knockdown of SCS-ATP and SCS-GTP in INS 832/13 cells and rat islets

In order to influence metabolism-induced changes in mtGTP cells and islets were transfected with siRNA to silence each of the SCS isoforms that operate in parallel in the TCA cycle. By

silencing SCS-ATP (ΔSCS-ATP) mtGTP production rates would be expected to increase by diversion of succinyl-CoA generated by oxoglutarate dehydrogenase to SCS-GTP (Fig. 1B). Likewise, silencing of SCS-GTP (ΔSCS-GTP) would lead to diminished mtGTP production (Fig. 1C). Unlike mtATP, silencing will primarily influence mtGTP because mtGTP is trapped within the matrix. Baseline mRNA levels demonstrated the SCS-GTP message was 6.0 ± 0.4 compared to SCS-ATP in INS 832/13 cells and 6.1 ± 1.2 in rat islets. Forty-eight hours following siRNA transfection SCS-ATP mRNA decreased by 50% and SCS-GTP mRNA by 90% while the untargeted isoform was not effected (Fig. 2A). Similar results were observed with a second set of siRNA to non-overlapping mRNA sequences and a non-specific siRNA had no effect on either isoform (data not shown). When cultured rat islets were transfected with the first set of siRNA the ATP-isoform was suppressed by 30% and the GTP-isoform by 50% (Fig. 2B). This degree of silencing was less compared to INS cells and was accompanied by a significant increase in the message of the untargeted isoform such that the SCS-ATP/SCS-GTP mRNA ratios were similar for cultured cells and islets. To confirm that the effects of mRNA silencing also occurred at the protein level, enzyme activities of each isoform were measured in mitochondrial lysates from transfected INS cells (Fig. 2C). Following siRNA-mediated silencing of SCS-ATP, the ratio of SCS-GTP/SCS-ATP activity increased 50% while silencing SCS-GTP reduced the ratio by half.

In order to examine whether SCS silencing influenced substrate-level nucleoside triphosphate synthesis within the mitochondrial matrix oligomycin and dinitrophenol (DNP) were added to intact mitochondrial from INS cells (Fig. 2D). Oligomycin inhibits ATP synthesis by the F1/F0 ATP synthase and DNP uncouples ΔΨ that both reduces ATP synthesis and relieves feedback inhibition from accumulation of reduced NADH. The GTP/ATP synthesis rate in mitochondria from ΔSCS-ATP cells measured in this manner exhibited a trend towards an increase, while there was a 55% reduction in the GTP/ATP rate from ΔSCS-GTP mitochondria again confirming the effect of silencing.

## mtGTP regulates insulin secretion in INS 832/13 cells and rat islets

Mitochondria are central to the mechanism of GSIS by both canonical and non-canonical pathways. To assess the significance of mtGTP as an intramitochondrial energy sensor, GSIS was measured in INS 832/13 cells and rat islets following silencing. SCS silencing modestly altered basal insulin secretion with secretion variably elevated for ΔSCS-ATP and variably decreased for ΔSCS-GTP in INS cells (Fig. 3A). The enhanced basal secretion of ΔSCS-ATP cells suppressed to levels of controls with 250 uM diazoxide (not shown). The most pronounced impact of mtGTP on insulin secretion was observed 90 minutes after stimulation with 15 mM glucose. GSIS in ΔSCS-ATP cells nearly doubled while in ΔSCS-GTP cells secretion was reduced 50%. The same observations were made when the difference between basal and stimulated secretion was compared (Fig. 3B). Similar results were observed also using a second set of siRNA against each isoform while a non-specific siRNA had no effect and KCl-induced secretion in ΔSCS-GTP cells was indistinguishable from that of controls (not shown). The potent salutary effect of mtGTP on insulin secretion was also confirmed in cultured rat islets (Fig. 3C and D). The same bidirectional response to glucose occurred despite reduced silencing in islets emphasizing the importance of the mtGTP signal to normal GSIS.

## mtGTP-mediated insulin secretion is coupled to cytosolic calcium

Because cytosolic calcium triggers insulin secretion in both canonical and non-canonical pathways, the effects of SCS silencing were assessed on stimulated cytosolic calcium. The average basal and stimulated cytosolic calcium assessed by fura-2 AM correlated directly with insulin secretion: large increases in both basal and stimulated calcium in ΔSCS-ATP cells, and no stimulated change for ΔSCS-GTP cells (Fig. 4 A and B). Removing extracellular calcium

completely blocked GSIS (Fig. 4C). Diazoxide maintains the $K_{ATP}$ channel in the open configuration and completely inhibited GSIS in control cells and substantially reduced GSIS in ΔSCS-ATP cells indicating that mtGTP-mediated effects were dependent, at least in part, on plasma membrane depolarization. Nifedipine, a potent inhibitor of plasma membrane L-type VDCC, reduced insulin secretion by 56 ± 4% in controls and 36 ±13% in ΔSCS-ATP cells (Fig 4D). In contrast, verapamil, an inhibitor of both the VDCC and ryanodine receptors (RYR), more potently reduced insulin secretion in ΔSCS-ATP cells (84 ± 5 %) but had no additional effect on control cells suggesting enhanced mtGTP signaling also requires mobilization of intracellular calcium stores (Valdivia et al., 1990).

### mtGTP-mediated insulin secretion is non-canonical

Two components define canonical insulin secretion: first mitochondrial metabolism leads to an increase in ATP and the ATP/ADP ratio and second this increase leads to closure of the $K_{ATP}$ channel with subsequent depolarization activation of VDCCs. To assess glucose-stimulated $K_{ATP}$-independent insulin secretion, cells were treated with diazoxide and then depolarized with 30 mM KCl in the presence of 3 or 15 mM glucose (Fig. 5A). Basal and stimulated insulin secretion was enhanced in the ΔSCS-ATP cells despite pharmacological elimination of the $K_{ATP}$ channels.

The expected increases in whole-cell [ATP], [GTP], ATP/ADP, and GTP/GDP ratios were observed with glucose stimulation of control cells (Figs. 5B-D). Except for a lower basal ATP, similar results were seen in [ATP], [GTP], ATP/ADP, GTP/GDP in ΔSCS-GTP cells despite poor GSIS. ΔSCS-ATP cells, on the other hand, had reduced basal and stimulated nucleoside triphosphate levels and tri- to diphosphate ratios as well as lacking a significant increase following stimulation despite enhanced insulin secretion. These changes, in particular for ΔSCS-ATP cells that have enhanced insulin secretion, are inconsistent with changes in ATP and ATP/ADP predicted by the canonical mechanism that requires an increase in the ATP/ADP ratio to close $K_{ATP}$ channels.

### mtGTP influences mitochondrial energy consumption and ΔΨ

Glucose-stimulated changes in oxygen consumption, cellular NAD(P)H, and ΔΨ were investigated to identify metabolic links between mtGTP and cytosolic calcium. Oxygen consumption assesses mitochondrial electron transport up to complex IV prior to ATP synthesis by F1/F0 ATP synthase. Oxygen consumption was not adversely affected by silencing of either SCS isoform confirming that SCS isoforms operate in parallel in the TCA cycle (Fig. 6A). Glucose stimulation increased oxygen consumption by ~20% in control and both ΔSCS-ATP and ΔSCS-GTP cells. The hyper-responsive ΔSCS-ATP cells, however, had significantly elevated basal and stimulated oxygen consumption compared to control reflecting higher overall rates of fuel consumption. Similar increases in basal oxygen consumption and basal insulin secretion have also previously been observed in MIN6 cells lacking SIRT4 (Haigis et al., 2006). Reduced pyridine nucleotides supply the electron transport chain to generate ΔΨ and consume oxygen. Basal concentrations of NAD(P)H measured by auto-fluorescence in living cells were all similar (Fig. 6B). Glucose-stimulated NAD(P)H was 35% lower in ΔSCS-ATP cells compared to stimulated control and ΔSCS-GTP cells consistent with the observed increased oxygen consumption rates.

A concordant increase in ΔΨ was observed in glucose-stimulated control cells as measured by TMRE fluorescence (Fig. 6C). In contrast to the increased rates of oxygen consumption, in the ΔSCS-ATP cells ΔΨ was not augmented by glucose consistent with an increased expenditure of the energy of oxidation. Furthermore, while ΔSCS-GTP cells had similar oxygen consumption as control cells, ΔΨ was significantly increased suggesting lower ΔΨ expenditure.

### mtGTP influences oxidative phosphorylation and mitochondrial calcium

Either increased ATP consumption or reduced ATP production could account for lower cellular purine triphosphates in the setting of increased oxygen consumption, increased NAD(P)H oxidation, and ΔΨ expenditure observed in the hyper-secreting ΔSCS-ATP cells. To examine this question directly ATP synthetic rates were assessed by $^{31}$P magnetic resonance spectroscopy in alginate-entrapped INS cells that were perifused in an NMR probe. Unidirectional ATP synthesis was calculated by saturation transfer of the γ-phosphate of ATP (Jucker et al., 2000). Basal ATP synthesis rates were similar for all three groups of entrapped cells (Fig. 7A). However, only control and ΔSCS-GTP cells augmented ATP synthesis rates when provided with 15 mM glucose. Instead of increasing ATP synthesis rates beyond that of controls, ΔSCS-ATP cells had only minimal response to glucose. Thus the lower cellular levels of ATP are from decreased ATP synthesis rather than increased ATP consumption.

ΔSCS-ATP cells have lower rates of ATP synthesis in the setting of higher rates of mitochondrial oxygen consumption and ΔΨ utilization suggesting other sites of energy usage in these cells. In contrast, ΔSCS-GTP cells have normal oxygen consumption and ATP synthesis but excess energy remaining in ΔΨ. Another high capacity mechanism consuming ΔΨ, aside from uncoupling to produce heat, includes the export of calcium from the mitochondrial matrix. The influence of mtGTP on glucose-stimulated increases in mitochondrial calcium was measured in INS EK-3 cells with mitochondrial-targeted aequorin (Fig. 7B) since mitochondrial calcium transport is essential for GSIS (Kennedy et al., 1996). Glucose-stimulated increases in mtGTP were similar between control and ΔSCS-ATP cells but ΔSCS-GTP cells had increased mitochondrial calcium suggesting that the calcium became trapped in the matrix and could not be transported out despite an increased ΔΨ.

## Discussion

Mitochondria coordinate fuel metabolism with insulin secretion. Here we present evidence that mtGTP is an important signal involved in mediating GSIS. Substrate-level synthesis of mtGTP by SCS-GTP produces GTP at a rate directly proportional to TCA cycle flux. Increases in the rate of GTP synthesis by reducing the expression of SCS-ATP results in increased oxygen consumption and cytosolic calcium with a concomitant increase in insulin secretion, which is unassociated with an increase in the ATP/ADP ratio or NAD(P)H. Conversely, if GTP synthesis is decreased by silencing SCS-GTP then oxygen consumption, ATP synthesis, and NAD(P)H levels increase while cytosolic calcium does not leading to impaired GSIS. Taken together these data suggest that TCA cycle-generated mtGTP regulates insulin secretion by increasing cytosolic calcium.

Glucose is the primary physiological secretagogue for pancreatic β-cells and in this setting glucokinase is the rate-controlling step for GSIS. However, non-glycolytically-derived fuels can support stimulated insulin secretion emphasizing the central importance of mitochondrial metabolism. Mitochondria from Rho$^0$ cells lack mitochondrial DNA encoded subunits of complexes I, III, IV, and V and lack fuel-stimulated insulin secretion but not depolarization-induced insulin secretion identifying requirement of electron transport for GSIS (Kennedy et al., 1998;Noda et al., 2002). Electron transport is necessary but not sufficient for insulin secretion since cytosolic oxidation of glycerophosphate (solely by providing $FADH_2$ to complex II) failed to induce insulin secretion despite generating ΔΨ (Antinozzi et al., 2002;Maechler et al., 1997). Mitochondrial oxidation of glycerophosphate or succinate by the TCA cycle, however, can both stimulate insulin secretion suggesting another component besides the transmembrane potential is necessary for this process (Antinozzi et al., 2002).

In this study, we sought to identify whether there was a signaling role for mtGTP in addition to GDH regulation. While the energy of hydrolysis of the γ-phosphate of GTP and ATP are the same, in the cytosol ATP tends to behave more as a fuel (except in the allosteric regulation of it's own synthesis), whereas GTP tends to be involved in cell signaling cascades (e.g. via G-proteins). A notable exception, somewhat unique to β-cells, is the regulation of the $K_{ATP}$/SUR channel by the ATP/ADP ratio though cytosolic GTP and GDP may also have a role (Bokvist et al., 1991;Dunne and Petersen, 1986). mtATP is primarily produced via oxidative phosphorylation prior to its rapid transport in exchange for ADP. ATP synthesis rates are proportional to oxidative phosphorylation but not necessarily to TCA flux (e.g. diversion of ΔΨ for heat production in brown adipose). In contrast, mtGTP in addition to being independent of ΔΨ is an isolated pool with only limited exchange with the cytosol. Little is known about the mechanism of guanine nucleotide transport across the mitochondria inner membrane but in cardiac myocytes it has been shown to be slow compared to ATP and ADP and appears to be independent of the ATP/ADP translocase (McKee et al., 1999;McKee et al., 2000). Yeast lack SCS-GTP and have a mitochondrial GTP/GDP translocase but no homolog in higher organisms has yet been identified (Vozza et al., 2004). In addition, the non-diffusible GTP pool from mouse islets only accounts for a small percent of total cellular GTP (Detimary et al., 1996). Thus, aside from the possibility of local or compartmentalized fluctuations, SCS-GTP does not appear to contribute significantly to the cellular GTP pool and suggests mtGTP exerts its influence within the mitochondria. This arrangement affords mtGTP at least three advantageous properties favorable to being an important intramitochondrial signal for TCA cycle activity: 1) direct coupling to TCA cycle flux, 2) independence from cytosolic nucleotide pools, and since GDP also has slow exchange 3) a greater dynamic range of the GTP/GDP ratio.

The relevance of mtGTP to β-cells is especially evident with the evoked insulin response to a glucose challenge. ΔSCS-ATP dramatically increased GSIS in both rat islets and INS 832/13 cells while ΔSCS-GTP dramatically decreased insulin secretion. Preserved oxygen consumption, KCl-stimulated secretion, nucleoside triphosphate levels, and NAD(P)H levels in ΔSCS-GTP cells indicate that the lack of GSIS was from the loss of the mtGTP signal. This bidirectional response with respect to the SCS-GTP to SCS-ATP ratio is strong supporting evidence that mtGTP is the operational signal observed in these experiments.

The more responsive ΔSCS-ATP cells demonstrated increased oxygen consumption and lower NAD(P)H levels consistent with increased energy fuel consumption and energy expenditure. In contrast to canonical $K_{ATP}$-dependent pathway of insulin secretion, here we show that the mtGTP signal leads to increased cytosolic calcium independent of the ATP/ADP ratio. The unidirectional rate constant for ATP synthesis was measured in living INS cells to determine whether this lack of increase of ATP in ΔSCS-ATP cells despite increased oxidation was due to both increased ATP synthesis and metabolism or rather decreased ATP synthesis. The lack of a change in ATP synthesis in the setting of increased fuel consumption suggests that ΔΨ was consumed by some energy utilizing process involved with insulin secretion. $K_{ATP}$-independence was further demonstrated by enhanced GSIS in the presence of diazoxide and depolarizing concentrations of KCl.

Mitochondria require several crucial elements to integrate fuel sensing with insulin secretion. First, mitochondrial metabolism by the TCA cycle via both direct and anaplerotic (notably pyruvate carboxylation) pathways are involved in the generation of some second messenger (MacDonald et al., 2005). Second, this fuel must be metabolized to deliver reduced NADH for oxidation to Complex I, as delivering reducing equivalents via the Complex II-dependent glycerophosphate shuttle fails to stimulate insulin secretion (Antinozzi et al., 2002;Maechler et al., 1997). Next, generation of ΔΨ is required and the degree of hyperpolarization correlates

tightly with insulin secretion while proton uncouplers disrupt secretion (Antinozzi et al., 2002). A portion of ΔΨ is utilized by ATP synthesis to close $K_{ATP}$ channels and supply the cells energy needs. Another portion of ΔΨ drives calcium out of the matrix via $Na^+$-dependent and independent shuttles in the inner mitochondrial membrane. Finally, mitochondrial calcium uptake and release correlates with and is essential for physiologic insulin secretion (Kennedy et al., 1996;Kennedy and Wollheim, 1998;Lee et al., 2003;Maechler et al., 1997). Indeed these studies identified that mitochondrial calcium increases in response to glucose are both earlier and larger than those of calcium in the cytosol.

Matrix sequestration and release of calcium as well as mitochondrial-mediated interactions with plasma membrane and endoplasmic reticulum calcium channels are well-established effectors of cytosolic calcium (Parekh, 2003;Rizzuto et al., 2004). These ΔΨ-dependent mitochondrial calcium fluctuations are well documented in insulin-secreting cells and associated with insulin release (Kennedy et al., 1996;Kennedy and Wollheim, 1998;Lee et al., 2003). Matrix calcium is a well-known activator of TCA dehydrogenases and pharmacologic inhibition of mitochondrial calcium efflux increases both cytosolic and matrix calcium as well as insulin secretion while inhibition of calcium influx inhibits insulin secretion (Lee et al., 2003;Maechler et al., 1997). Mitochondrial calcium translocation also consumes ΔΨ and is thus a candidate process to account for the observed discrepancy between oxygen usage and ATP synthesis. In ΔSCS-GTP cells the increased ΔΨ and increased mitochondrial calcium suggest that low mtGTP prevents efficient export of calcium out of the matrix. In ΔSCS-ATP cells where mtGTP is elevated, increased oxygen consumption with a reduced ΔΨ and lower ATP production rates suggest that energy may have been diverted from ATP synthesis to enhance mitochondria calcium export. The observations from SCS silencing are consistent with mtGTP-induced changes in distribution of ΔΨ from ATP synthesis into calcium partitioning and not primarily by calcium stimulation of matrix dehydrogenases. The differential efficacy of verapamil and nifedipine raise the prospect of RyR involvement in mtGTP signaling. At present, the mechanism for the mtGTP signal is unknown and further work will be needed to clarify how it regulates cytosolic calcium. Given that ER calcium regulation by the RyR influences insulin secretion, that both RyR and VDAC are localized to contacts sites between the mitochondria and ER, and that mitochondrial calcium efflux may occur via the channel formed between VDAC and the AAT makes this an attractive mechanism to coordinate mitochondrial metabolism with cytosolic calcium (Brdiczka et al., 2006;Hajnoczky et al., 2002;Islam, 2002;Rapizzi et al., 2002;Szalai et al., 2000).

The metabolic relationship between glucose and mtGTP in β-cells is stoichiometric. A consequence of this fidelity is that the energy of glucose metabolism can be harnessed to drive proportionate insulin-releasing calcium oscillations. An advantage of this arrangement would allow β-cells to remain responsive to TCA flux even when there is a surfeit of energy and metabolites. Taken together these findings describe a fundamental role for mtGTP to coordinate mitochondrial metabolism with glucose-induced insulin secretion.

## Experimental Procedures

### Materials and Cell Culture

Fluorophores were purchased from Molecular Probes (Eugene, OR) and all other chemicals were purchased from Sigma (St. Louis, MO) unless otherwise specified. Protein measurements were performed using BCA protein reagent (Pierce; Rockford, IL) in a 96-microwell format. Initial stocks of clonal INS-1 832/13 cells, over-expressing the human insulin gene were a kind gift from Dr. Christopher B. Newgard (Duke University School of Medicine; Durham, NC) (Hohmeier et al., 2000). Cells were cultivated as monolayers in RPMI 1640 with 11.1 mM D-glucose supplemented with 10% (v/v) fetal bovine serum, antibiotics (10,000 units/ml

penicillin and 10 mg/ml streptomycin), 10 mM HEPES, 2 mM L-glutamine, and 1 mM sodium pyruvate, and 50 uM β-mercaptoethanol. EK-3 cells also had G418 at 150 ug/ml in the media (Kennedy et al., 1996). Islets were isolated from 250–300 g Sprague Dawley rats by standard procedures from the DERC core facility by collagenase digestion and hand picking four times. Islets were cultured in 100 mm dishes with RPMI 1640 with 3 mM glucose, 10% fetal bovine serum and antibiotics (10,000 units/ml penicillin and 10 mg/ml streptomycin). Cultures were maintained at 37°C under humidified (5% $CO_2$, 95% air) conditions and cells used between passages 10 and 60.

## RNAi Transfections

Cells were transfected using RNAifect (Qiagen; Valencia, CA) as per manufacturers recommendation with the following ratios: 3–6 ul siRNA (20 uM), 9 ul transfection reagent, 100 ul buffer EC-R, and 1 ml of Opti-MEM 1 with Glutamax (GIBCO Invitrogen Corporation, Carlsbad, CA). Eight to 24 hours following transfections the culture media was then changed back to RPMI 1640. Cells were used within 2–3 days following transfection. RNAi complexes for islets were prepared using Gene Silencer (Genlantis, Sandiego, CA) using 4.5–9 ul of siRNA (20 uM) and 18 ul of transfection reagent per ml of culture media as per manufacturers recommendation. Islets were transfected following overnight culture by first transferring them to Opti-MEM and overlaying transfection complexes. 8–12 hours later an equal volume of culture media was added to the islets then used 24–36 hours following transfection. Transfection efficiency in INS cells was estimated to be reproducibly ~90% in INS cells and about 60% in islets with varying potency unique to each individual siRNA. siRNA were synthesized by Qiagen with 5 prime dTdT overhangs as follows: ΔSCS-ATP: #1 AAATGGTGCTGGCTTGGCTAT and #2 AAGGTACACGAGTTGATGATG and ΔSCS-GTP: #1 AAGGTGATGGTTGCTGAAGCC and #2 CAGCAGATGATTGGTTATAAT. Control Luciferase GL2 duplex siRNA was purchased from Dharmacon (Lafayette, CO).

## mRNA Quantitiation

Total RNA was extracted using RNeasy with RNase-Free DNase (Qiagen) from 6-well plates or batches of 15–20 medium sized islets following 2 days of transfection. Reverse transcriptase reactions were performed separately on a PTC-100 Thermocycler (BioRad, Hercules, CA) using Stratascript reverse transcriptase (Stratagene; La Jolla, CA), prior to real time PCR analysis on an Opticon 2 DNA Engine (BioRad) using Quantitect Probe PCR reagent (Qiagen). All reactions confirmed a single product of the expected size by agarose gel electrophoresis. Reaction efficiencies for actin, SCS-ATP and SCS-GTP were greater than 1.90. ΔSCS isoform mRNA levels were expressed as percent of actin (%Actin = $E_{SCS}^{C(t)SCS}/E_{Actin}^{C(t)Actin} * 100$) or as the ΔΔC(t) normalized to actin, where E is efficiency of the steady state reaction and C (t) is the cycle threshold. Primers were synthesized at the Yale School of Medicine HHMI/ Keck facility and TaqMan internal fluorophore-quencher pairs were synthesized by Applied Biosystems as follows: Actin CCAGATCATGTTTGAGACCTTC, CATGAGGTAGTCTGTCAGGTCC, VIC-AGCCATGTACGTAGCCATCCAGGCT-TAMRA; SCS-ATP TGTGGTACGGTTACAAGGTACA, ACAACCATTTTAGCAGCTTCAT, FAM-TGCTAAGGCACTAATTGCAGACAGTGG-TAMRA; SCS-GTP GAGGAAGAGGAAAAGGTGTCTT, TCTAGAAATATCCAGGGCTTCA, FAM-ATCATCTGCTGAGCCAGCTGTCCC-TAMRA

## Purine Nucleotide Measurements

Samples were dissolved in 50% acetonitrile with 10 mM spermine and 4 μls were injected into an API 3000 LC/MS/MS (PE Sciex, Foster City, CA) equipped with turbo ion spray and

measured as previously described for cell lysates (Cline et al., 2004). ATP, ADP, GTP, GDP and taurine were simultaneously measured and the signal was normalized to known standards calibrated by their extinction coefficients.

### Mitochondria Isolation

Cells from four confluent 100 mm dishes per condition were washed with PBS prior to being scraped in ice-cold mitochondrial isolation buffer (65 mM Sucrose, 215 mM Mannitol, 5 mM $KH_2PO_4$, 5 mM $KHCO_3$, 3 mM $MgCl_2$, 5 mM Hepes pH 7.4). Cells were spun at 1000 rcf for 5 minutes and lysates were made from the resuspended pellet with 40 strokes of Type B pestle in a 2 ml glass dounce homogenizer. Lysates were centrifuged for 3 minutes at 1800 rcf and then the supernatant was centrifuged at 10,800 rcf for an additional 3 minutes. The mitochondria-enriched pellet was again resuspended in isolation buffer and low and high-speed spins were repeated.

### SCS Enzyme Activities

Mitochondria were disrupted by hypotonic swelling in 20 mM HEPES, 3 mM $MgCl_2$, and 0.2 mM taurine pH 7.4. To maintain internal consistency, mitochondria from the same pool were assayed for both SCS isoform activities in the reverse direction. Reactions were started with the addition of mitochondrial extracts to pre-warmed reaction buffer (37° C) for final concentrations of 10 mM succinate, 500 μM coenzyme A and 500 μM ATP or GTP. Aliquots were collected at specified time intervals and quenched in ice cold 50% acetonitrile with 0.05% trifluoroacetic acid and 10 mM spermine. Reactions were monitored by LC/MS/MS as the appearance of succinyl CoA in negative ion mode selecting for the m-1 of the intact molecule in the first quadrapole and the 408.3 Da fragment in the last quadrapole. Data were normalized to the taurine standard and expressed in either arbitrary units per minute or as ratios of GTP to ATP activity.

### Mitochondrial SCS Nucleotide Production Rates

The rates of accumulation of ATP and GTP were measured *simultaneously* in intact mitochondria supplied with 10 mM succinate, 500 μM ADP and GDP. Reactions were initiated with the addition the substrates to mitochondrial isolation buffer with a final concentration of substrate, 200 μM taurine (internal standard) with 10 μg/ml oligomycin and 100 μM DNP. Aliquots were quenched with ice cold 50% acetonitrile. Succinate was used as an anaplerotic substrate for these reactions (requiring forward metabolism via the TCA cycle to produce succinyl CoA) (MacDonald et al., 2005). The combination of oligomycin with an uncoupler avoids altering NADH/NAD and ATP/ADP ratios (LaNoue et al., 1972;LaNoue and Williamson, 1971). Succinate as substrate activates succinate dehydrogenase and allows for the SCS step to be rate limiting for treated and untreated mitochondria (Kearney, 1957). Mitochondrial GDP uptake is slow in comparison to ADP, but was not rate limiting under these reaction conditions. Individual reaction rates were calculated as the percent production of NTP from NDP per minute $100*(\Delta NTP/(NDP+NTP))/\Delta t$ under steady state conditions as measured by LC/MS/MS and reported as the ratio of individual isoform activities or absolute activities in arbitrary units.

### Insulin Secretion

Confluent cells in 6-well plates were washed with phosphate buffered saline (PBS) and then pre-incubated in KRBH (129 mM NaCl. 4.8 mM KCl, 1.2 mM $KH_2PO_4$, 1.2 mM $MgSO_4$, 2 mM $CaCl_2$, 20 mM HEPES and 24 mM $NaHCO_3$ gassed with 95% $O_2$/5%$CO_2$) with 0.2% 96% fatty acid-free bovine serum albumin and 3 mM dextrose for 2 hours. Media was then changed to KRBH with additions as specified and incubated for indicated times. The NaCl

concentration was reduced accordingly when depolarizing with KCl to maintain osmolarity. Nifedipine, verapamil, or diazoxide cells were preincubated for 15 minutes in basal glucose prior to stimulation. Fractions were collected on ice and spun at 1800 rcf for 5 minutes at 4 ° C. The remaining media was aspirated and cells were washed with PBS x2 and then 1 ml of ice cold 0.1% Triton X 100 was added. Cell lysates were collected and assayed for protein. siRNA-transfected islets were transferred to KRBH with 2.5 mM glucose and incubated for 2 hours. 10–12 islets per well were then transferred to fresh media with 2.5 mM glucose and a t = 0 sample was immediately collected. Following a 45-minute incubation a second aliquot was taken and a volume of KRBH equal to that remaining added to bring to glucose concentration to 15 mM. Following the second 45 minute incubation the media and islets were separately collected. Basal secretion was the difference between time 0 and 45 minutes. Stimulated secretion is the difference between the insulin 90 minutes and at the 45-minutes time point × 0.5. Insulin was measured by immunoassays in 96-well plates (ALPCO Diagnostics, Windham, NH).

### NAD(P)H measurements

Transfected cells were grown in T150 flasks to confluence, trypsin digestioned and quenched with media containing 10% FBS. Cells were then pelleted at low speed and washed twice in KRBH with 3 mM glucose. Cells were diluted into either buffer containing 3 mM or 15 mM glucose and allowed to equilibrate for 30 minutes in a 37° C water bath. Autofluorescence was measured on a Hitachi F-3010 fluorescence spectrophotometer equipped with temperature control with excitation at 280 nm (5 nm bp) and emission 348 nm (5 nm bp) for tryptophan and 340 nm (10 nm bp) excitation and 470 nm (20 nm bp) emission for NAD(P)H.

### Mitochondrial membrane potential and calcium measurements

Cells were grown to confluence in 96 well plates and read on a Victor$^3$ multilabel plate counter (Perkin Elmer, Boston, MA). For membrane potential measurements cells were incubated in KRBH with 3 mM glucose and labeled with 0.1 ng/ml Hoechst 33342 for 30 minutes in the incubator. The media was changed to either 3 mM or 15 mM glucose incubated another 30 minutes. TMRE was then added to the wells to a final concentration of 1 pM and incubated an additional 15 minutes before immediately reading at 355 nm excitation and 460 nm emission for Hoechst 33342 and 570 nm excitation and 620 nm emission for TMRE. For static cytosolic calcium measurements fura-2 AM was loaded in INS cells for 45 minutes in basal media with 1 mM probenecid to prevent cellular extrusion in the presence of glucose (Arkhammar et al., 1989). Following 2 washes cells were incubated for 15 minutes in 3 mM or 15 mM glucose and immediately read with excitation at 340 and 380 nm and emission at 510 nm (Chroma Technology Corp., Rockingham, VT). Concentrations were calculated using an intracellular Kd of 280 nM with cells incubated in 0.01% Triton X 100 with either 3 mM EGTA or 1 mM $CaCl_2$. Kinetic measurements were performed at room temperature following the addition of basal or stimulatory glucose with measurements every 100 seconds for 340 and 380 nm excitations. Static mitochondrial calcium measurements were obtained using EK-3 cells (Kennedy et al., 1996) loaded with coelenterazine-hcp reconstituted in 2-hydroxypropyl-β-cyclodextrin at 1 ug/ml in basal KRBH for 45 minutes before changing media to basal or stimulatory glucose for 15 minutes. Luminescence was read immediately 2 seconds per well.

### Oxygen Consumption

Cells from 3–4 confluent wells of a 6-well plate were collected by trypsinization, washed, and resuspended in KRBH with 3 mM glucose, stained with trypan blue and then manually counted. Oxygen consumption was measured as previously described using 5–7.5×$10^6$ cells in air-tight 650 ul custom made titanium chambers (Instech Laboratories; Plymouth Meeting, PA)

maintained at 37 °C (Papas and Jarema, 1998). Cells were suspended by stirring and glucose was added without the addition of any outside air. Oxygenation was detected with fiber optic probes impregnated with a sodium hydrosulfite-calibrated fluorophore quenched by oxygen and detected with Model 210 Fiber optic Oxygen Monitor and data collected and processed by Ocean Optics OOI Sensor v. 1.00.08 (Instech).

### NMR studies of mitochondrial ATP production

An AVANCE™ 500 NMR spectrometer (Bruker Instruments, Inc, Billerica, MA) was used with the bioreactor placed within the bore of a 10mm dual-channel broad-band probe. Cell viability was determined by measuring ATP and intracellular $P_i$, concentrations, and pH from the $^{31}$P-NMR spectrum of the entrapped cells. $P_i$ concentrations of control and SCS-silenced cells were similar for basal and stimulatory measurements. ATP synthesis rates were determined by $^{31}$P-NMR saturation-transfer techniques, and calculated from the change in intensity of $P_i$ when the $\gamma$-$PO_4$ of ATP is irradiated with a frequency selective radiofrequency pulse, and the $T_1$ relaxation time of $P_i$ during $\gamma$-$PO_4$ saturation similar to that described in skeletal muscle (Jucker et al., 2000). Control spectra with the saturation pulse centered equidistant downfield from $P_i$ were interleaved with the $\gamma$-$PO_4$ saturation pulse. Data have unidirectional rate constants minimum set to 0 that eliminated negative mathematical artifacts and did not change the relative differences between basal and stimulated states. A drop in the unidirectional rate constant in the presence of DNP confirmed the lack of an artifact from contributions to apparent ATP synthesis by glyceraldehyde-3 phosphate dehydrogenase and phosphoglycerate kinase .

**Perifusion Protocol—**Entrapped cells were perifused in the bioreactor in the bore of the NMR spectrometer. $^{31}$P-NMR spectra were acquired during step changes in metabolic substrates and inhibitors, and collected in 20-minute experiments for each substrate level. Substrate concentrations were manipulated by addition of substrate to the perifusate reservoir, thereby ensuring thorough mixing and temperature and oxygen equilibration of the media before reaching the bioreactor.

**Bioreactor/NMR Spectrometer—**To achieve the high cell density necessary for adequate signal to noise at reasonable time intervals, we use a packed bed perifusion bioreactor loaded with either phantom alginate beads, or alginate beads with entrapped cells. The perifusion system was equipped with a combined heat and gas exchanger for temperature and oxygen level adjustment, and flow-through cells for temperature and oxygen concentration measurements. Oxygen partial pressures were measured using a Clark-type polarographic oxygen sensor. These features enable the maintenance and monitoring of well-oxygenated cells within the bore of the NMR spectrometer at physiological pH and temperature.

**Alginate Encapsulation Procedure—**Cells were entrapped in alginate beads of approximately 3 mm in diameter. Beads were prepared by nebulization of a homogeneous alginate (3% w/v) –cell (~$10^8$ cells/ml) suspension into a 1.1% $BaCl_2$ solution, where polymerization of the alginate entraps the cells in a matrix that allows free diffusion of soluble compounds and proteins. The beads were incubated in a sterile spinner flask until ready for use. The mild conditions of the entrapment procedure yield beads that contain highly viable and functional cells. Between 60 and 80 beads were used for each experiment for a total of approximately $3 \times 10^7$ cells per experiment. Nucleotide concentrations were reported as mM for the entire sampled volume (including both extra- and intracellular volumes) and not as the intracellular concentrations.

### Statistics and Data Analysis

All data are reported as mean ± S.E. Unpaired two-tailed Student's t-tests, One-way ANOVA with a Tukey post-test comparison, or Two-way ANOVA with Bonferonni post test comparisons were performed using Prism software package v. 4 (GraphPad; San Diego, CA). Differences were considered statistically significant at $p < 0.05$.

#### Acknowledgements

We would like to thank Jenny Taylor, Siobahn Skowronek, Nicole Prestiano, Xiaojian Zhao, and Debra Mento for expert technical assistance. Islet isolations were preformed by Tamara Dlugos as a service of the Y.U. Diabetes Endocrine Research Core (DERC). This work was supported by Public Health Service grants R01 DK-71071, P01 DK-68229, R01 DK-40936, P30 DK-45735, and U24 DK-76169. G.I.S. is the recipient of a Distinguished Clinical Scientist Award from the American Diabetes Association.

## References

Antinozzi PA, Ishihara H, Newgard CB, Wollheim CB. Mitochondrial metabolism sets the maximal limit of fuel-stimulated insulin secretion in a model pancreatic beta cell: a survey of four fuel secretagogues. Journal of Biological Chemistry 2002;277:11746–11755. [PubMed: 11821387]

Arkhammar P, Nilsson T, Berggren PO. Glucose-stimulated efflux of fura-2 in pancreatic beta-cells is prevented by probenecid. Biochem Biophys Res Commun 1989;159:223–228. [PubMed: 2647080]

Bokvist K, Ammala C, Ashcroft FM, Berggren PO, Larsson O, Rorsman P. Separate processes mediate nucleotide-induced inhibition and stimulation of the ATP-regulated K(+)-channels in mouse pancreatic beta-cells. Proc Biol Sci 1991;243:139–144. [PubMed: 1676517]

Brdiczka DG, Zorov DB, Sheu SS. Mitochondrial contact sites: their role in energy metabolism and apoptosis. Biochim Biophys Acta 2006;1762:148–163. [PubMed: 16324828]

Cline GW, LePine RL, Papas KK, Kibbey RG, Shulman GI. 13C NMR Isotopomer Analysis of Anaplerotic Pathways in INS-1 Cells. Journal of Biological Chemistry 2004;279:44370–44375. [PubMed: 15304488]

Detimary P, Jonas JC, Henquin JC. Stable and diffusible pools of nucleotides in pancreatic islet cells. Endocrinology 1996;137:4671–4676. [PubMed: 8895332]

Dunne MJ, Petersen OH. GTP and GDP activation of K+ channels that can be inhibited by ATP. Pflugers Arch 1986;407:564–565. [PubMed: 2431387]

Fraser ME, James MN, Bridger WA, Wolodko WT. Phosphorylated and dephosphorylated structures of pig heart, GTP-specific succinyl-CoA synthetase. J Mol Biol 2000;299:1325–1339. [PubMed: 10873456]

Haigis MC, Mostoslavsky R, Haigis KM, Fahie K, Christodoulou DC, Murphy AJ, Valenzuela DM, Yancopoulos GD, Karow M, Blander G, et al. SIRT4 inhibits glutamate dehydrogenase and opposes the effects of calorie restriction in pancreatic beta cells. Cell 2006;126:941–954. [PubMed: 16959573]

Hajnoczky G, Csordas G, Yi M. Old players in a new role: mitochondria-associated membranes, VDAC, and ryanodine receptors as contributors to calcium signal propagation from endoplasmic reticulum to the mitochondria. Cell Calcium 2002;32:363–377. [PubMed: 12543096]

Hohmeier HE, Mulder H, Chen G, Henkel-Rieger R, Prentki M, Newgard CB. Isolation of INS-1-derived cell lines with robust ATP-sensitive K+ channel-dependent and -independent glucose-stimulated insulin secretion. Diabetes 2000;49:424–430. [PubMed: 10868964]

Islam MS. The ryanodine receptor calcium channel of beta-cells: molecular regulation and physiological significance. Diabetes 2002;51:1299–1309. [PubMed: 11978625]

Johnson JD, Mehus JG, Tews K, Milavetz BI, Lambeth DO. Genetic evidence for the expression of ATP- and GTP-specific succinyl-CoA synthetases in multicellular eucaryotes. Journal of Biological Chemistry 1998;273:27580–27586. [PubMed: 9765291]

Jucker BM, Dufour S, Ren J, Cao X, Previs SF, Underhill B, Cadman KS, Shulman GI. Assessment of mitochondrial energy coupling in vivo by 13C/31P NMR. Proceedings of the National Academy of Sciences of the United States of America 2000;97:6880–6884. [PubMed: 10823916]

Kearney EB. Studies on succinic dehydrogenase. IV. Activation of the beef heart enzyme. J Biol Chem 1957;229:363–375. [PubMed: 13491588]

Kelly A, Stanley CA. Disorders of glutamate metabolism. Mental Retardation & Developmental Disabilities Research Reviews 2001;7:287–295. [PubMed: 11754524]

Kennedy ED, Maechler P, Wollheim CB. Effects of depletion of mitochondrial DNA in metabolism secretion coupling in INS-1 cells. Diabetes 1998;47:374–380. [PubMed: 9519742]

Kennedy ED, Rizzuto R, Theler JM, Pralong WF, Bastianutto C, Pozzan T, Wollheim CB. Glucose-stimulated insulin secretion correlates with changes in mitochondrial and cytosolic Ca2+ in aequorin-expressing INS-1 cells. Journal of Clinical Investigation 1996;98:2524–2538. [PubMed: 8958215]

Kennedy ED, Wollheim CB. Role of mitochondrial calcium in metabolism-secretion coupling in nutrient-stimulated insulin release. Diabetes & Metabolism 1998;24:15–24. [PubMed: 9534004]

Kowluru A. Adenine and guanine nucleotide-specific succinyl-CoA synthetases in the clonal beta-cell mitochondria: implications in the beta-cell high-energy phosphate metabolism in relation to physiological insulin secretion. Diabetologia 2001;44:89–94. [PubMed: 11206416]

LaNoue KF, Bryla J, Williamson JR. Feedback interactions in the control of citric acid cycle activity in rat heart mitochondria. J Biol Chem 1972;247:667–679. [PubMed: 4333508]

LaNoue KF, Williamson JR. Interrelationships between malate-aspartate shuttle and citric acid cycle in rat heart mitochondria. Metabolism 1971;20:119–140. [PubMed: 4322086]

Lee B, Miles PD, Vargas L, Luan P, Glasco S, Kushnareva Y, Kornbrust ES, Grako KA, Wollheim CB, Maechler P, et al. Inhibition of mitochondrial Na+-Ca2+ exchanger increases mitochondrial metabolism and potentiates glucose-stimulated insulin secretion in rat pancreatic islets. Diabetes 2003;52:965–973. [PubMed: 12663468]

MacDonald MJ, Fahien LA, Brown LJ, Hasan NM, Buss JD, Kendrick MA. Perspective: emerging evidence for signaling roles of mitochondrial anaplerotic products in insulin secretion. American Journal of Physiology - Endocrinology & Metabolism 2005;288:E1–15. [PubMed: 15585595]

MacMullen C, Fang J, Hsu BY, Kelly A, de Lonlay-Debeney P, Saudubray JM, Ganguly A, Smith TJ, Stanley CA. Hyperinsulinism/hyperammonemia Contributing I. Hyperinsulinism/hyperammonemia syndrome in children with regulatory mutations in the inhibitory guanosine triphosphate-binding domain of glutamate dehydrogenase. Journal of Clinical Endocrinology & Metabolism 2001;86:1782–1787. [PubMed: 11297618]

Maechler P, Kennedy ED, Pozzan T, Wollheim CB. Mitochondrial activation directly triggers the exocytosis of insulin in permeabilized pancreatic beta-cells. EMBO Journal 1997;16:3833–3841. [PubMed: 9233793]

McKee EE, Bentley AT, Smith RM Jr, Ciaccio CE. Origin of guanine nucleotides in isolated heart mitochondria. Biochemical & Biophysical Research Communications 1999;257:466–472. [PubMed: 10198236]

McKee EE, Bentley AT, Smith RM Jr, Kraas JR, Ciaccio CE. Guanine nucleotide transport by atractyloside-sensitive and -insensitive carriers in isolated heart mitochondria. American Journal of Physiology - Cell Physiology 2000;279:C1870–1879. [PubMed: 11078702]

Noda M, Yamashita S, Takahashi N, Eto K, Shen LM, Izumi K, Daniel S, Tsubamoto Y, Nemoto T, Iino M, et al. Switch to anaerobic glucose metabolism with NADH accumulation in the beta-cell model of mitochondrial diabetes. Characteristics of betaHC9 cells deficient in mitochondrial DNA transcription. J Biol Chem 2002;277:41817–41826. [PubMed: 12169697]

Ottaway JH, McClellan JA, Saunderson CL. Succinic thiokinase and metabolic control. International Journal of Biochemistry 1981;13:401–410. [PubMed: 6263728]

Papas KK, Jarema MA. Glucose-stimulated insulin secretion is not obligatorily linked to an increase in O2 consumption in betaHC9 cells. American Journal of Physiology 1998;275:E1100–1106. [PubMed: 9843754]

Parekh AB. Store-operated Ca2+ entry: dynamic interplay between endoplasmic reticulum, mitochondria and plasma membrane. J Physiol 2003;547:333–348. [PubMed: 12576497]

Rapizzi E, Pinton P, Szabadkai G, Wieckowski MR, Vandecasteele G, Baird G, Tuft RA, Fogarty KE, Rizzuto R. Recombinant expression of the voltage-dependent anion channel enhances the transfer of Ca2+ microdomains to mitochondria. J Cell Biol 2002;159:613–624. [PubMed: 12438411]

Rizzuto R, Duchen MR, Pozzan T. Flirting in little space: the ER/mitochondria Ca2+ liaison. Sci STKE 2004;2004:re1. [PubMed: 14722345]

Smith CM, Bryla J, Williamson JR. Regulation of mitochondrial alpha-ketoglutarate metabolism by product inhibition at alpha-ketoglutarate dehydrogenase. Journal of Biological Chemistry 1974;249:1497–1505. [PubMed: 4361738]

Szalai G, Csordas G, Hantash BM, Thomas AP, Hajnoczky G. Calcium signal transmission between ryanodine receptors and mitochondria. J Biol Chem 2000;275:15305–15313. [PubMed: 10809765]

Szollosi A, Nenquin M, Aguilar-Bryan L, Bryan J, Henquin JC. Glucose stimulates Ca2+ influx and insulin secretion in 2-week-old beta-cells lacking ATP-sensitive K+ channels. J Biol Chem 2007;282:1747–1756. [PubMed: 17138557]

Valdivia HH, Valdivia C, Ma J, Coronado R. Direct binding of verapamil to the ryanodine receptor channel of sarcoplasmic reticulum. Biophys J 1990;58:471–481. [PubMed: 2169916]

Vozza A, Blanco E, Palmieri L, Palmieri F. Identification of the mitochondrial GTP/GDP transporter in Saccharomyces cerevisiae. Journal of Biological Chemistry 2004;279:20850–20857. [PubMed: 14998997]

Weitzman PD, Jenkins T, Else AJ, Holt RA. Occurrence of two distinct succinate thiokinases in animal tissues. FEBS Letters 1986;199:57–60. [PubMed: 3956747]

Wolodko WT, Fraser ME, James MN, Bridger WA. The crystal structure of succinyl-CoA synthetase from Escherichia coli at 2.5-A resolution. J Biol Chemv 1994;269:10883–10890.

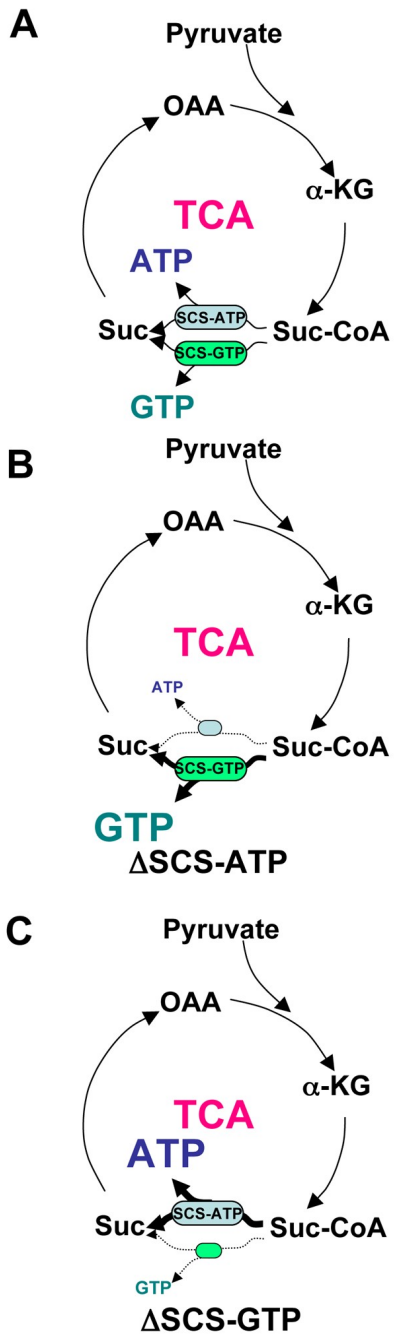


**Figure 1. Schematic of mtGTP production**

**A)** Pyruvate from glycolysis supplies carbon to the TCA cycle that is subsequently metabolized to succinyl-CoA. Succinyl-CoA is enzymatically converted to succinate and either ATP by SCS-ATP or GTP by SCS-GTP.

**B**) SCS-ATP silencing (ΔSCS-ATP) leads to diversion of TCA flux through SCS-GTP to increase mtGTP.

**C**) SCS-GTP silencing (ΔSCS-GTP) reduces flux through SCS-GTP resulting in lower mtGTP production.

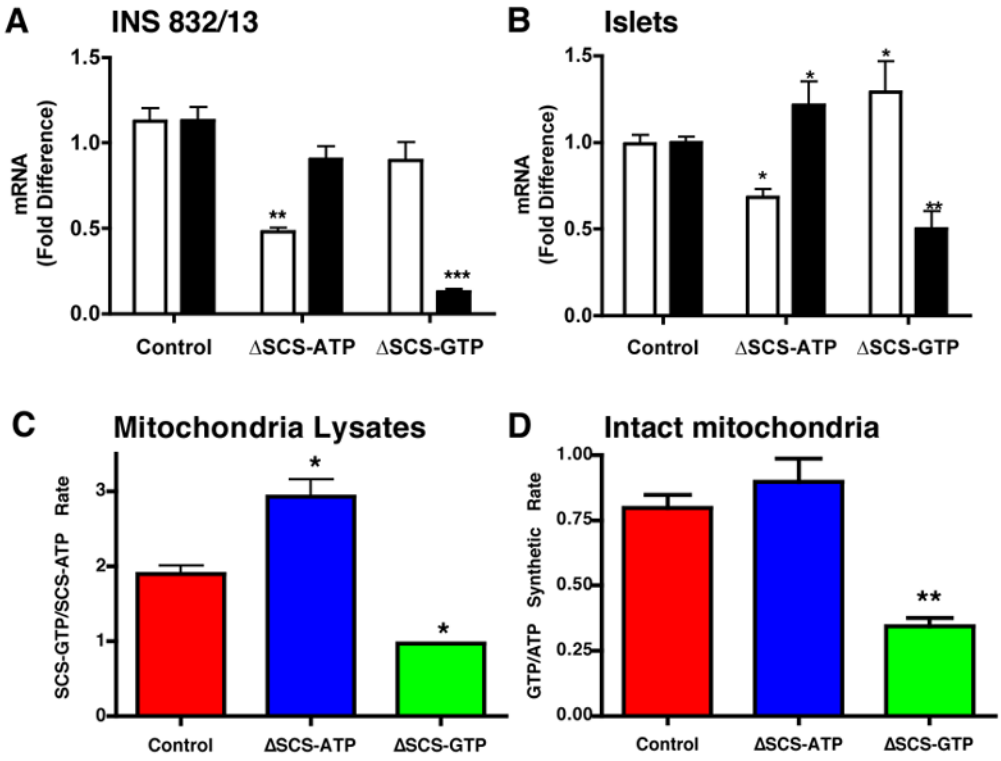


**Figure 2. Silencing of SCS-ATP and SCS-GTP in INS 832/13 cells and rat islets**

**A** and **B**) Fold change in SCS-ATP (white) and SCS-GTP (black) in INS 832/13 cells (n=4) (**A**) and rat islets (n=5) (**B**) 48 hours following transfection with siRNA against SCS-ATP or SCS-GTP.

**C** and **D** ) Ratio of SCS-GTP to SCS-ATP enzyme activities in mitochondrial extracts (**C**) and intact mitochondria treated with 10 μg/ml oligomycin and 100 μM DNP (**D**) isolated from control (red), ΔSCS-ATP (blue), and ΔSCS-GTP (green) cells (n=3). Error bars show mean ± SEM; ANOVA: *, $p<0.05$; **, $p<0.01$; *** $p<0.001$ vs. control.

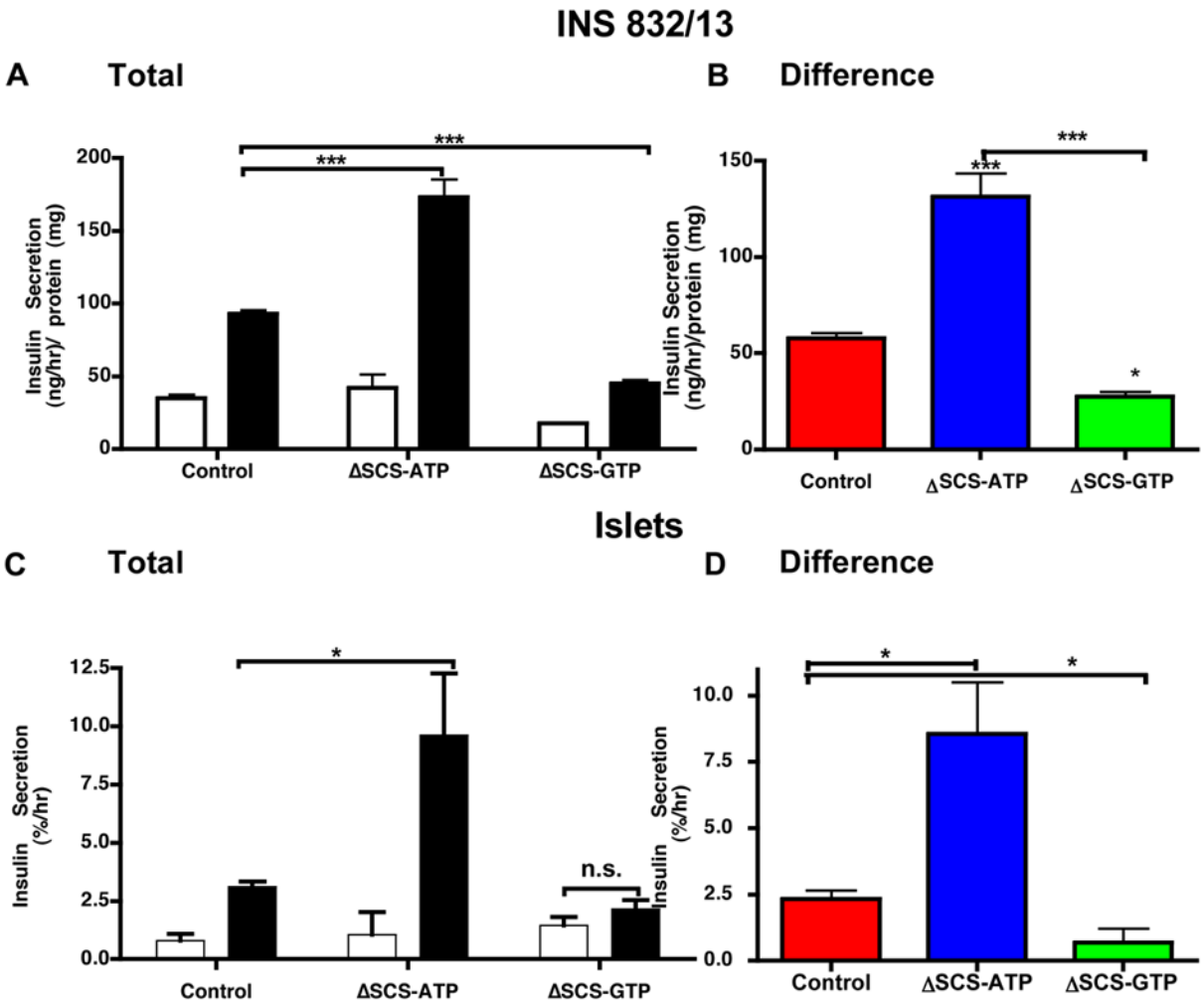


**Figure 3. Stimulated insulin secretion in SCS isoform silenced INS cells and rat islets**

Static insulin secretion assays were performed in (**A** and **B**) INS 832/13 cells (n=8) or (**C** and **D**) rat islets (n=6 with ~11 islets/replicate) for 90 minutes following siRNA transfection in 3 mM (white) and 15 mM (black) glucose. (**B** and **D**) show the difference in insulin secretion between basal and stimulation for each group. Error bars show mean ± SEM; ANOVA: *, $p<0.05$; **, $p<0.01$; ***, $p<0.001$ compared to controls. For all groups basal vs. stimulated insulin secretion was statistically significant (t-test) unless otherwise shown (n.s. = not significant).

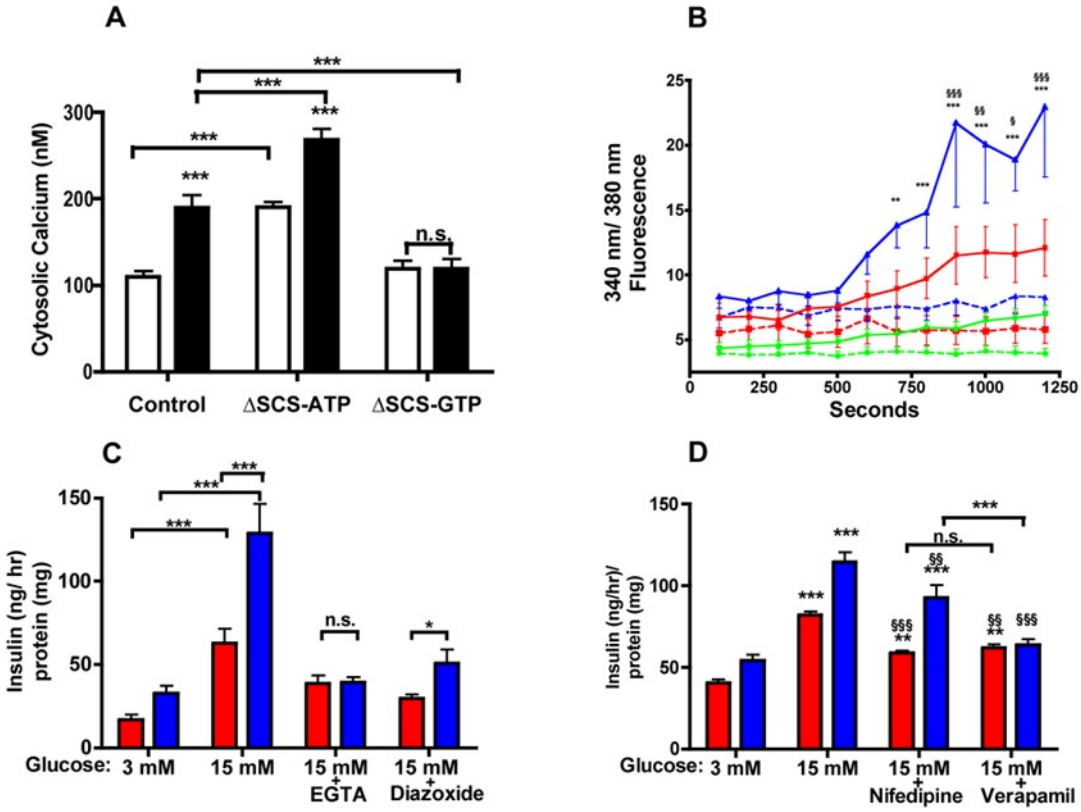


**Figure 4. mtGTP-mediated insulin secretion is cytosolic calcium-dependent**

**A**) Cytosolic calcium concentration determined by fura-2 AM labeling of control, ΔSCS-ATP, and ΔSCS-GTP INS cells following 30 minutes of stimulation with 3 mM (white) or 15 mM (black) glucose (n=10).

**B**) The ratio of 340 nm/380 nm fluorescence over time of control (red square), ΔSCS-ATP (blue triangle), and ΔSCS-GTP (green circle) cells loaded with fura-2 AM and stimulated with either 3 mM (broken) or 15 mM (solid) glucose (n=8).

**C, D**) Insulin secretion in control (red) and ΔSCS-ATP (blue) cells in basal or stimulatory media (**C**) plus 250 μM diazoxide or 3 mM EGTA for 45 minutes (n=6) or (**D**) plus 20 uM nifedipine or 100 μM verapamil for 2 hours (n=6).

Error bars show mean ± SEM; 2-way ANOVA **, p<0.01; *** p<0.001 vs. control unless otherwise indicated. §, P<0.05; §§, p<0.01; §§§ p<0.001 vs. stimulated.

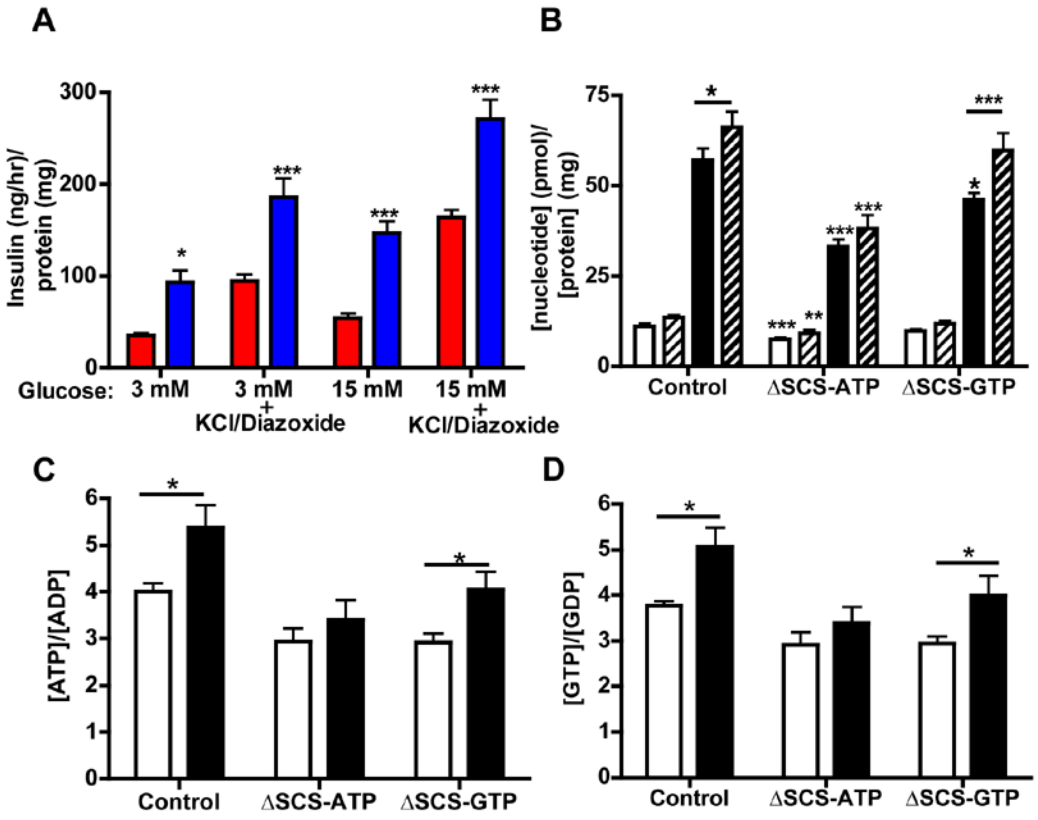


**Figure 5. mtGTP is a non-canonical signal for GSIS**

**A**) Insulin secretion following stimulation for 45 minutes with 15 mM glucose ± 30 mM KCl and 250 μM Diazoxide (n=6) for control (red) and ΔSCS-ATP (blue) cells (n=6). Significance is shown vs. controls.

**B**) Whole-cell concentration of GTP (white) and ATP (black) from control, ΔSCS-ATP, and ΔSCS-GTP cells in 3 mM (open) and 15 mM (hatched) glucose. Significance is vs. controls unless otherwise indicated (n=12).

**C** and **D**) Ratios of **C**) ATP/ADP and **D**) GTP/GDP ratio from control, ΔSCS-ATP, and ΔSCS-GTP cells in 3 mM (white) and 15 mM (black) glucose. Significance is shown vs. the basal state (n=12).

Error bars show mean ± SEM; 2-way ANOVA or t-test between basal and stimulation: *, $p<0.05$; **, $p<0.01$; *** $p<0.001$ vs. control unless otherwise stated.

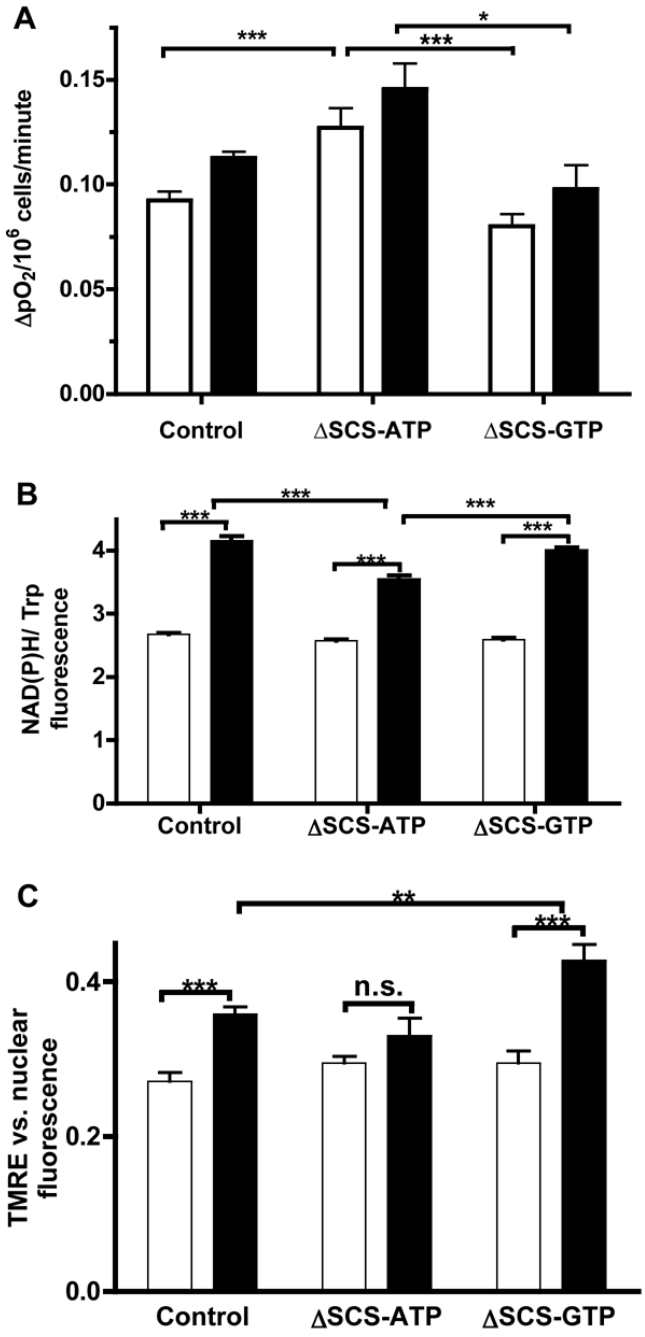


**Figure 6. mtGTP effects on oxygen consumption, NADPH oxidation, and ΔΨ**

**A**) Oxygen consumption rates of suspended cells at 3 mM (white) and 15 mM (black) glucose following silencing of SCS (n=14 basal and n=5 stimulation).

**B**) Cellular NAD(P)H in response to 3 mM (white) and 15mM (black) glucose as measured by the ratio of NAD(P)H to tryptophan autofluorescence in suspended cells (n=4).

**C**) Mitochondrial membrane potential in response to 3 mM (white) and 15 mM (black) glucose as measured by the ratio of fluorescence of TMRE (ΔΨ) vs. Hoescht 33342 (nuclear) (n=14). Error bars show mean ± SEM; ANOVA: *, $p<0.05$; **, $p<0.01$; *** $p<0.001$ compared to controls unless otherwise indicated.

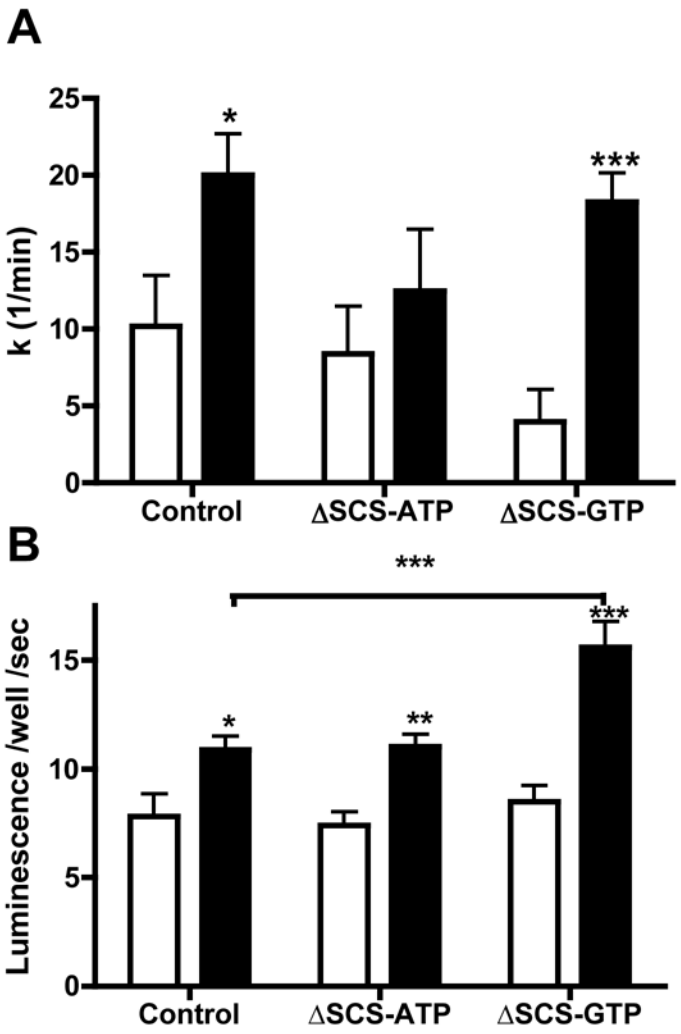


**Figure 7. mtGTP alters the balance between ATP synthesis and mitochondrial calcium export**

**A)** *In vivo* ATP synthesis rates in entrapped and perfused control, ΔSCS-ATP, and ΔSCS-GTP cells in 3 mM (white) and 15 mM (black) glucose as determined by saturation transfer of ATP gamma $^{31}$P. Significance is shown vs. the basal state (n=6).

**B**) Mitochondrial calcium concentration determined by aequorin luminescence in INS EK-3 cells in control, ΔSCS-ATP, and ΔSCS-GTP cells following 15 minutes of stimulation with 3 mM (white) or 15 mM (black) glucose.

Error bars show mean ± SEM; ANOVA:*, $p<0.05$; **, $p<0.01$; *** $p<0.001$ compared to controls unless otherwise indicated.